

A high-significance detection of non-Gaussianity in the WMAP 3-year data using directional spherical wavelets

J. D. McEwen,^{1*} M. P. Hobson,¹ A. N. Lasenby¹ and D. J. Mortlock²

¹*Astrophysics Group, Cavendish Laboratory, J. J. Thomson Avenue, Cambridge CB3 0HE, UK*

²*Blackett Laboratory, Imperial College of Science, Technology and Medicine, Prince Consort Road, London SW7 2BW, UK*

13 April 2006

ABSTRACT

We repeat the directional spherical real Morlet wavelet analysis used to detect non-Gaussianity in the Wilkinson Microwave Anisotropy Probe (WMAP) 1-year data (McEwen et al. 2005a), on the WMAP 3-year data. The non-Gaussian signal previously detected is indeed present in the 3-year data, although the significance of the detection is reduced. Using our most conservative method for constructing significance measures, we find the significance of the detection of non-Gaussianity drops from $98.3 \pm 0.4\%$ to $94.9 \pm 0.7\%$; the significance drops from $99.3 \pm 0.3\%$ to $97.2 \pm 0.5\%$ using a method based on the χ^2 statistic. The wavelet analysis allows us to localise most likely sources of non-Gaussianity on the sky. We detect very similar localised regions in the WMAP 1-year and 3-year data, although the regions extracted appear more pronounced in the 3-year data. When all localised regions are excluded from the analysis the 3-year data is consistent with Gaussianity.

Key words: cosmic microwave background – methods: data analysis – methods: numerical

1 INTRODUCTION

Recent measurements of the cosmic microwave background (CMB) anisotropies, in particular those made by the Wilkinson Microwave Anisotropy Probe (WMAP), provide data of unprecedented precision with which to study the origin of the universe. Such observations have led strong support to the standard cosmological concordance model. Nevertheless, many details and assumptions of the concordance model are still under close scrutiny. One of the most important and topical assumptions of the standard model is that of the statistics of the primordial fluctuations that give rise to the anisotropies of the CMB. In the simplest inflationary models, primordial perturbations seed Gaussian temperature fluctuations in the CMB that are statistically isotropic over the sky. However, this is not necessarily the case for non-standard inflationary models or various cosmic defect scenarios.

The assumptions of Gaussianity and isotropy have been questioned recently with many works highlighting deviations from Gaussianity in the WMAP 1-year data (WMAP1; Bennett et al. 2003), calculating measures such as the bispectrum and Minkowski functionals (Komatsu et al. 2003; Magueijo & Medeiros 2004; Land & Magueijo 2005a; Medeiros & Contaldi 2005), the genus (Colley & Gott 2003; Eriksen et al. 2004), correlation functions (Gaztanaga & Wagg 2003; Eriksen et al. 2005; Tojeiro et al. 2006), low-multipole alignment statistics (de Oliveira-Costa et al. 2004; Copi et al. 2004, 2005; Schwarz et al. 2004; Slosar & Seljak 2004; Weeks 2004; Land & Magueijo 2005b,c,d,e; Bielewicz et al. 2005;

de Oliveira-Costa & Tegmark 2006), structure alignment statistics (Wiaux et al. 2006) phase associations (Chiang et al. 2003; Chiang & Naselsky 2004; Coles et al. 2004; Dineen et al. 2005), local curvature (Hansen et al. 2004; Cabella et al. 2005), the higher criticism statistic (Cayón et al. 2005), hot and cold spot statistics (Larson & Wandelt 2004, 2005), fractal statistics (Sadegh Movahed et al. 2006) and wavelet coefficient statistics (Vielva et al. 2003; Mukherjee & Wang 2004; McEwen et al. 2005a,c; Cruz et al. 2005, 2006a). Some statistics show consistency with Gaussianity, whereas others provide some evidence for a non-Gaussian signal and/or an asymmetry between the northern and southern Galactic hemispheres. Although the recently released WMAP 3-year data (WMAP3; Hinshaw et al. 2006) is consistent with the WMAP1 data, a more thorough treatment of beams, foregrounds and systematics in the 3-year data, in addition to a further two years of observing time, mean that WMAP3 provides a more reliable data-set on which to confirm or refute previous results. A Gaussianity analysis is performed on the WMAP3 data by Spergel et al. (2006), using the one point distribution function, Minkowski functionals, the bispectrum and the trispectrum. No evidence is found for non-Gaussianity, however the authors do not re-evaluate the large number of statistical tests that have been used to detect non-Gaussianity in the WMAP1 data. Indeed, deviations from Gaussianity and isotropy have recently been detected in the WMAP3 data, using measures such as anisotropy statistics (Helling et al. 2006; Bernui et al. 2006) phase associations (Chiang et al. 2006) and wavelet coefficient statistics (Cruz et al. 2006b), with little change in the significance levels obtained by each technique for the first and third year data. Although the departures from Gaussianity and isotropy detected in the WMAP1 and

* E-mail: mcewen@mrao.cam.ac.uk

WMAP3 data may simply highlight unremoved foreground contamination or other systematics, which itself is of importance for cosmological inferences drawn from the data, if the source of these detections is of cosmological origin then this would have important implications for the standard cosmological model.

In this letter we focus on the significant detection of non-Gaussianity that we made previously in the WMAP1 data using directional spherical wavelets (McEwen et al. 2005a), to see if the detection is still present in the WMAP3 data. The remainder of this letter is organised as follows. In Section 2 we briefly review the analysis procedure and discuss the data maps considered. Results are presented and discussed in Section 3, before concluding remarks are made in Section 4.

2 NON-GAUSSIANITY ANALYSIS

We repeat on the WMAP3 data our non-Gaussianity analysis performed previously on the WMAP1 data (McEwen et al. 2005a), focusing only on the most significant detection of non-Gaussianity made previously. We refer the reader to our previous work (McEwen et al. 2005a) for a detailed description of the analysis procedure and present here only a very brief overview.

We apply a spherical wavelet analysis to probe the WMAP data for non-Gaussianity. Wavelets are an ideal tool to search for deviations from Gaussianity due to the scale and spatial localisation inherent in a wavelet analysis. To perform a wavelet analysis of full-sky CMB maps we apply our fast continuous spherical wavelet transform (CSWT; McEwen et al. 2005b), which is based on the spherical wavelet transform developed by Antoine, Vanderghyest and colleagues (Antoine & Vanderghyest 1998, 1999; Antoine et al. 2002, 2004; Wiaux et al. 2005) and the fast spherical convolution developed by Wandelt & Górski (2001). We use only the real Morlet wavelet in this analysis since it gave the most significant detection of non-Gaussianity in the WMAP1 data (McEwen et al. 2005a).

To minimise the contribution of foregrounds and systematics to CMB anisotropy measurements, the WMAP assembly contains a number of receivers that observe at a range of frequencies (Bennett et al. 2003). In this analysis we consider the signal-to-noise ratio enhanced co-added map constructed from the WMAP3 data. This map is constructed by the same procedure described generally by Komatsu et al. (2003) and described in the context of our non-Gaussian analysis by McEwen et al. (2005a). We use the foreground reduced sky maps and apply the Kp0 mask to remove residual Galactic emission and known point sources. The foreground maps and mask are available from the Legacy Archive for Microwave Background Data Analysis (LAMBDA) website¹.

To quantify the significance of any deviations from Gaussianity we perform 1000 Monte Carlo simulations. This involves simulating 1000 Gaussian co-added maps. Each simulated map is constructed in an analogous manner to the co-added map constructed from the data. A Gaussian CMB realisation is simulated from the theoretical power spectrum fitted by the WMAP team (the power spectrum we use is also available from LAMBDA). Measurements made by the various receivers are then simulated by convolving with realistic beams and adding anisotropic WMAP3 noise for each receiver. The simulated observations for each receiver are then combined to give a co-added map.

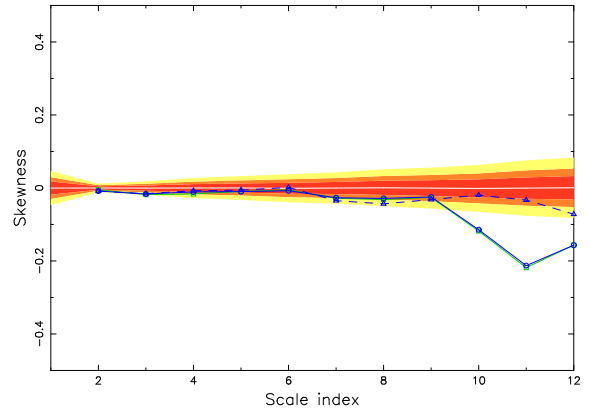


Figure 1. Real Morlet wavelet coefficient skewness statistics ($\gamma = 72^\circ$). Points are plotted for the WMAP1 data (solid, green, squares), WMAP3 data (solid, blue, circles) and the WMAP3 data with localised regions removed (dashed, blue, triangles). Confidence regions obtained from 1000 WMAP3 Monte Carlo simulations are shown for 68% (red), 95% (orange) and 99% (yellow) levels, as is the mean (solid white line).

To probe the WMAP3 data for deviations from Gaussianity the skewness of the real Morlet wavelet coefficients is examined over a range of scales and orientations (the scales and orientations considered are defined in McEwen et al. 2005a). Any deviation from zero is an indication of non-Gaussianity in the data. An identical analysis is performed on the 1000 Gaussian simulations to quantify the significance of any deviations.

3 RESULTS

The skewness of the real Morlet wavelet coefficients of the co-added WMAP3 map are displayed in Figure 1, with confidence intervals constructed from the 1000 WMAP3 Monte Carlo simulations also shown. Only the plot corresponding to the orientation of the maximum deviation from Gaussianity is shown. The non-Gaussian signal present in the WMAP1 data is clearly present in the WMAP3 data. In particular, the large deviation on scale $a_{11} = 550'$ and orientation $\gamma = 72^\circ$ is almost identical (although it is in fact very marginally lower in the WMAP3 data).

Next we consider in more detail the most significant deviation from Gaussianity on scale $a_{11} = 550'$ and orientation $\gamma = 72^\circ$. Figure 2 shows histograms of this particular statistic constructed from the WMAP1 and WMAP3 Monte Carlo simulations. The measured statistic for the WMAP1 and WMAP3 data is also shown on the plot, with the number of standard deviations each observation deviates from the mean of the appropriate set of simulations. The distribution of this skewness statistic is not significantly altered between simulations consistent with WMAP1 or WMAP3 data. The observed statistics for the WMAP1 and WMAP3 data are similar but the slightly lower value for WMAP3 is now more apparent.

To quantify the statistical significance of the detected deviation from Gaussianity we consider two techniques. The first technique involves comparing the deviation of the observed statistic to all statistics computed from the simulations. This is a very conservative means of constructing significance levels. The second technique involves performing a χ^2 test. In both of these tests we relate the observation to all test statistics originally computed, i.e.

¹ <http://cmbdata.gsfc.nasa.gov/>

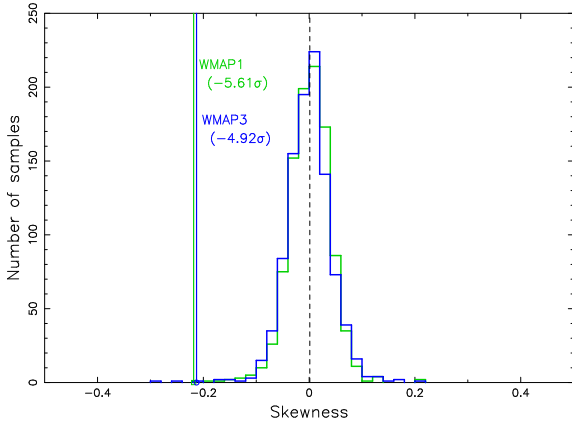


Figure 2. Histograms of real Morlet wavelet coefficient skewness ($a_{11} = 550'$; $\gamma = 72^\circ$) obtained from 1000 Monte Carlo simulations. Histograms are plotted for simulations in accordance with WMAP1 (green) and WMAP3 (blue) observations. The observed statistics for the WMAP1 and WMAP3 maps are shown by the green and blue lines respectively. The number of standard deviations these observations deviate from the mean of the appropriate set of simulations is also displayed.

to both skewness and kurtosis statistics². For a more thorough description of these techniques see McEwen et al. (2005a). Searching through the 1000 WMAP3 simulations, 51 maps have an equivalent or greater deviation than the WMAP3 data in any single test statistic computed for that map. Using the very conservative first technique, the significance of the detection of non-Gaussianity in the WMAP3 data may therefore be quoted at $94.9 \pm 0.7\%$ (an expression for the 1σ errors quoted on significance levels is derived in Appendix A). The distribution of χ^2 values obtained from the simulations is shown in Figure 3. The χ^2 value obtained for the data is also shown on the plot. The distribution of the χ^2 values is not significantly altered between simulations consistent with WMAP1 or WMAP3 data. The χ^2 value computed for the data, however, is significantly lower for the WMAP3 data. Computing the significance of the detection of non-Gaussianity directly from the χ^2 distribution and observation, the significance of the detection of non-Gaussianity in the WMAP3 data may be quoted at $97.2 \pm 0.5\%$. Using both of the techniques outlined above the significance of the detection of non-Gaussianity made with the WMAP3 data is slightly lower than that made with the WMAP1 data. Nevertheless, the non-Gaussian signal is still present at a significant level.

A wavelet analysis allows the spatial localisation of interesting signal characteristics. The most pronounced deviations from Gaussianity in the WMAP data may therefore be localised on the sky. The real Morlet wavelet coefficients of the WMAP3 data corresponding to the most significant detection of non-Gaussianity on scale $a_{11} = 550'$ and orientation $\gamma = 72^\circ$ are displayed in Figure 4. Thresholded wavelet coefficient maps for both the WMAP1 and WMAP3 data are also shown in order to localise the most pronounced deviations. The regions localised in the WMAP1 and WMAP3 data are very similar, although the localised regions appear slightly more pronounced, in the sense that the peaks are larger, in the WMAP3 data. To investigate the impact of localised regions on the initial detection of non-Gaussianity, the analysis is repeated with the WMAP3 localised regions excluded from the

² Although we recognise the distinction between skewness and kurtosis, there is no reason to partition the set of test statistics into skewness and kurtosis subsets. The full set of test statistics must be considered.

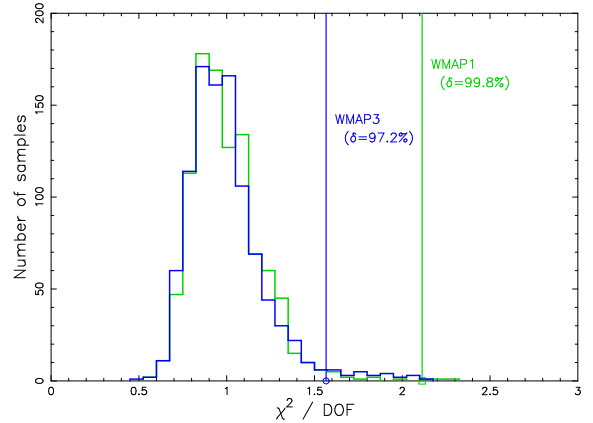


Figure 3. Histograms of normalised χ^2 test statistics computed from real Morlet wavelet coefficient statistics obtained from 1000 Monte Carlo simulations. Histograms are plotted for simulations in accordance with WMAP1 (green) and WMAP3 (blue) observations. The χ^2 value computed for the WMAP1 and WMAP3 maps are shown by the green and blue lines respectively. The significance of these observations, computed from the appropriate set of simulations, is also displayed.

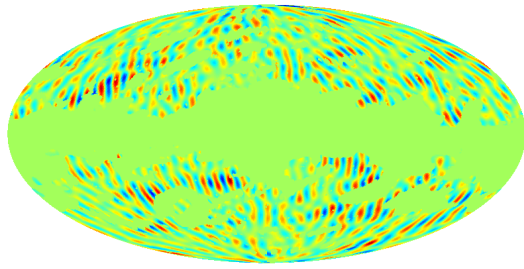
analysis. The resulting skewness statistics are shown by the dashed line in Figure 1. Interestingly, the highly significant detections of non-Gaussianity are eliminated when these localised regions are removed.

In our previous non-Gaussianity analysis (McEwen et al. 2005a) we also performed a preliminary noise analysis and found that noise was not atypical in the localised regions that we detect. The localised regions have not changed in the WMAP3 data, hence we do not expect this finding to change. In an additional work of ours (McEwen et al. 2005c) that investigated a Bianchi VII_h component as a possible source of non-Gaussianity – which, incidentally, we found not to be the predominant source of non-Gaussianity – we performed a preliminary analysis of foregrounds and systematics. We concluded that foregrounds or systematics were not the likely source of the detected non-Gaussianity. Again, we do not believe this finding to change in the WMAP3 data since both foregrounds and systematics are treated more thoroughly.

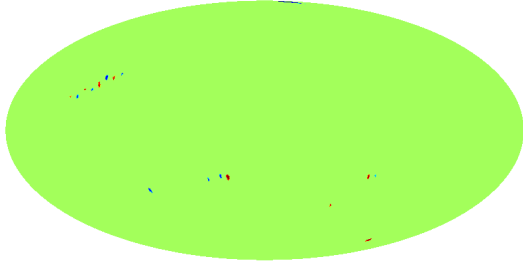
4 SUMMARY AND DISCUSSION

We have repeated on the WMAP3 data the directional spherical real Morlet wavelet analysis used to make a significant detection of non-Gaussianity in the WMAP1 data (McEwen et al. 2005a). The non-Gaussian signal previously detected is indeed present in the WMAP3 data, although the significance of the detection is reduced. Using our first very conservative method for constructing significance measures we find the significance of the detection of non-Gaussianity drops from $98.3 \pm 0.4\%$ to $94.9 \pm 0.7\%$. Using our second technique for constructing significance measures, which is based on a χ^2 analysis, the significance of the detection drops from $99.3 \pm 0.3\%$ to $97.2 \pm 0.5\%$. We have no intuitive explanation for this drop in significance.

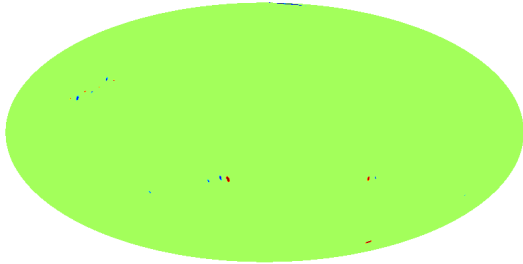
The most likely sources of non-Gaussianity were also localised on the sky. We detect the same regions in the WMAP3 data as found in the WMAP1 data, although the localised regions extracted appear slightly more pronounced in the WMAP3 data. When all localised regions are excluded from the analysis the data is consistent with Gaussianity. An interesting structure is extracted



(a) WMAP3 wavelet coefficients



(b) WMAP3 thresholded wavelet coefficients



(c) WMAP1 thresholded wavelet coefficients

Figure 4. Real Morlet spherical wavelet coefficient maps and thresholded versions ($a_{11} = 550'$; $\gamma = 72^\circ$). To localise most likely deviations from Gaussianity on the sky, the coefficient map is thresholded so that only those coefficients above 3σ (in absolute value) remain.

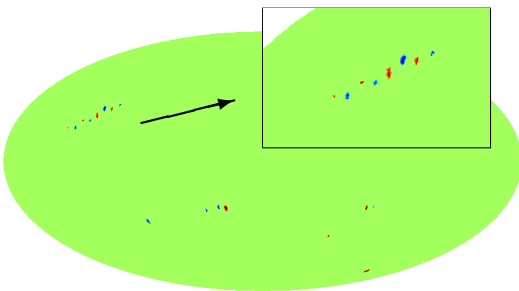


Figure 5. Thresholded real Morlet spherical wavelet coefficient map with localised regions inset ($a_{11} = 550'$; $\gamma = 72^\circ$).

in the north-west region of the thresholded maps (Figure 5). In a future work we intend to use optimal filters on the sphere, in conjunction with our fast CSWT analysis tool, to search for cosmic strings in the CMB, a possible source of the non-Gaussianity that we have detected in both the WMAP1 and WMAP3 data.

ACKNOWLEDGEMENTS

JDM thanks the Association of Commonwealth Universities and the Cambridge Commonwealth Trust for the support of a Commonwealth (Cambridge) Scholarship. Some of the results in this paper have been derived using the HEALPix package (Górski et al. 2005). We acknowledge the use of the Legacy Archive for Microwave Background Data Analysis (LAMBDA). Support for LAMBDA is provided by the NASA Office of Space Science.

REFERENCES

- Antoine J. -P., Murenzi R., Vanderghyest P., Ali S. T., 2004, Cambridge University Press, Cambridge
- Antoine J. -P. and Vanderghyest P., 1999, *Applied and Computational Harmonic Analysis*, 7, 1–30
- Antoine J. -P. and Vanderghyest P., 1998, *J. of Math. Phys.*, 39, 3987–4008
- Antoine J. -P., Demanet L., Jacques L., 2002, *Applied and Computational Harmonic Analysis*, 13, 3, 177–200
- Bielewicz P., Eriksen H. K., Banday A. J., Górski K. M., Lilje P. B., 2005, *ApJ*, 635, 750
- Bennett C. L. et al. (WMAP team), 2003, *ApJS*, 148, 1
- Bernui A., Mota B., Reboucas M. J., Tavakol R., 2006, preprint (astro-ph/0511666)
- Cabella P., Liguori M., Hansen F. K., Marinucci D., Matarrese S., Moscardini L., Vittorio N., 2005, *MNRAS*, 358, 684
- Cayón L., Jin J., Treaster A., 2005, *MNRAS*, 362, 826
- Chiang L. -Y., Naselsky P. D., Coles P., 2006, submitted to *ApJL* (astro-ph/0603662)
- Chiang L. -Y., Naselsky P. D., 2004, preprint (astro-ph/0407395)
- Chiang L. -Y., Naselsky P. D., Verkhodanov O. V., 2003, *ApJ*, 590, 65
- Colley W. N., Gott J. R., 2003, *MNRAS*, 344, 686
- Coles P., Dineen P., Earl J., Wright D., 2004, *MNRAS*, 350, 989
- Copi C. J., Huterer D., Starkman G. D., 2004, *Phys. Rev. D.*, 70, 043515
- Copi C. J., Huterer D., Schwarz D. J., Starkman G. D., 2005, submitted to *MNRAS* (astro-ph/0508047)
- Cruz M., Tucci M., Martínez-González E., Vielva P., 2006a, *MNRAS*, in press (astro-ph/0601427)
- Cruz M., Cayón L., Martínez-González E., Vielva P., Jin J., 2006b, submitted to *MNRAS* (astro-ph/0603859)
- Cruz M., Martínez-González E., Vielva P., Cayón L., 2005, *MNRAS*, 356, 29
- Dineen P., Rocha G., Coles P., 2005, *MNRAS*, 358, 1285
- Eriksen H. K., Banday A. J., Gorski K. M., Lilje P. B., 2005, *ApJ*, 622, 58
- Eriksen, H. K., Novikov, D. I., Lilje, P. B., Banday, A. J., Górski K. M., 2004, *ApJ*, 612, 64
- Gaztanaga E., Wagg J., 2003, *Phys. Rev. D.*, 68, 2130256
- Górski K. M., Hivon E., Banday A. J., Wandelt B. D., Hansen F. K., Reinecke M., Bartelmann M., 2005, *ApJ*, 622, 759
- Hansen F.K., Cabella P., Marinucci D., Vittorio N., 2004, *ApJL*, 607, L67
- Helling R. C., Schupp P., Tesileanu T., 2006, preprint (astro-ph/0603594)
- Hinshaw G. et al. (WMAP team), 2006, preprint (astro-ph/0603451)
- Komatsu E. et al., 2003, *ApJS*, 148, 119
- Land K., Magueijo J., 2005a, *MNRAS*, 357, 994

- Land K., Magueijo J., 2005b, MNRAS, 362, L16
 Land K., Magueijo J., 2005c, Phys. Rev. Lett., 95, 071301
 Land K., Magueijo J., 2005d, MNRAS, 362, 838
 Land K., Magueijo J., 2005e, Phys. Rev. D., 72, 101302
 Larson D. L., Wandelt B. D., 2004, ApJ, 613, 85
 Larson D. L., Wandelt B. D., 2005, submitted to Phys. Rev. D. (astro-ph/0505046)
 McEwen J. D., Hobson M. P., Lasenby A. N., Mortlock D. J., 2005a, MNRAS, 359, 1583
 McEwen J. D., Hobson M. P., Mortlock D. J., Lasenby A. N., 2005b, preprint (astro-ph/0506308)
 McEwen J. D., Hobson M. P., Lasenby A. N., Mortlock D. J., 2005c, MNRAS, in press (astro-ph/0510349)
 Magueijo J., Medeiros J., 2004, MNRAS, 351, L1
 Medeiros J., Contaldi C. R., 2005, MNRAS, 367, 39
 Mukherjee P., Wang Y., 2004, ApJ, 613, 51
 Sadegh Movahed M., Ghasemi F., Sohrab Rahvar, Reza Rahimi Tabar M., 2006, submitted to Phys. Rev. D. (astro-ph/0602461)
 Spergel D. N. et al. (WMAP team), 2006, preprint (astro-ph/0603449)
 de Oliveira-Costa A., Tegmark M., Zaldarriaga M., Hamilton A., 2004, Phys. Rev. D., 69, 63516
 de Oliveira-Costa A., Tegmark M., 2006, submitted to Phys. Rev. D. (astro-ph/0603369)
 Schwarz D. J., Starkman G. D., Huterer D., and Copi C. J., 2004, Phys. Rev. Lett., 93, 221301
 Slosar A., Seljak U., 2004, Phys. Rev. D., 70, 083002
 Tojeiro R., Castro P.G., Heavens A.F., Gupta S., 2006, MNRAS, 365, 265
 Vielva P., Martínez-González E., Barreiro R. B., Sanz J. L., Cayón L., 2003, ApJ, 609, 22
 Wandelt B. D., Górski K. M., 2001, Phys. Rev. D., 63, 123002, 1
 Weeks J., 2005, preprint (astro-ph/0412231)
 Wiaux Y., Jacques L., Vanderghenst P., 2005, ApJ, 632, 15
 Wiaux Y., Vielva P., Martínez-González E., Vanderghenst P., 2006, submitted to Phys. Rev. Lett. (astro-ph/0603367)

$$\sigma_{\hat{p}} = \left[-\frac{\partial^2 \ln \Pr(x|p)}{\partial p^2} \Big|_{p=\hat{p}} \right]^{-1/2} = \sqrt{\frac{x(n-x)}{n^3}}.$$

APPENDIX A: ERRORS ON SIGNIFICANCE LEVELS

In this appendix we derive the standard deviation of a significance level determined from Monte Carlo (MC) simulations. Suppose we perform n independent MC simulations. Let p denote the probability that an MC simulation chosen at random has a value for some test statistic that is larger than the corresponding value derived from the real data (hence p is the underlying significance we attempt to estimate). Choosing an MC simulation at random and defining whether it has a test statistic greater than that of the data thus corresponds to a Bernoulli trial with a probability of success equal to p .

Suppose we observe x successes in the n MC simulations. The likelihood for x is

$$\Pr(x|p) = {}^n C_x p^x (1-p)^{n-x}.$$

The maximum likelihood (ML) estimate \hat{p} of p is most easily given by maximizing the log-likelihood:

$$\frac{\partial \ln \Pr(x|p)}{\partial p} \Big|_{p=\hat{p}} = 0 \quad \Rightarrow \quad \hat{p} = \frac{x}{n},$$

which recovers the intuitive result. Approximating the shape of the likelihood near its peak by a Gaussian, we may approximate the standard deviation of \hat{p} by